CHAPTER V

DISCUSSION

5.1 Explanation of Abrasion Wear

5.1.1 Mechanism of abrasion wear by a simple model

First of all the simplistic model of abrasion wear by cone grits which is explained in the text book of "Engineering Tribology [45]" is introduced in order to understand the mechanism of abrasion wear. The model by a single grit is schematically illustrated in Fig.5-1.
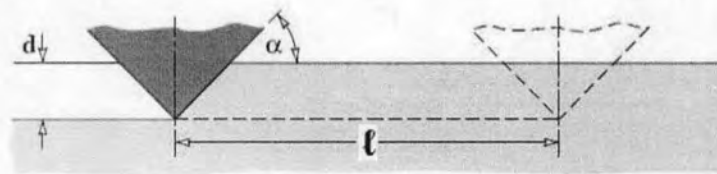

Fig5-1 Schematic drawing of model of abrasive wear by single grit.

According to the mathematical explanation by comparing this model with the formula of Vickers hardness formula (Eq.5-1), the individual load on a grit is the product of the multiplying the projected area of the indentation by the cone and the material's yield stress under indentation (hardness), as shown in Eq.5-2

$$F = AH_v \qquad\qquad (Eq.5-1)$$

where:

F : the force applied to the grit

A : the surface area of the resulting indentation

H_v : the Vickers hardness.

$$W_g = 0.5\pi(d\cot\alpha)^2 H \qquad\qquad (Eq.5-2)$$

where:

W_g : the individual load on a grit [N]

D : the depth of indentation [m]

α : the slope angle of the cone

H : the material's yield stress under indentation (hardness)

The approximate volume of the material removed by the cone is the product of the cross-sectional area of the indentation '$d^2\cot\alpha$' and the traversed distance 'ℓ', i.e.:

$$V_g = \ell d^2\cot\alpha \qquad \text{(Eq.5-3)}$$

where:

V_g : the volume of material removed by the cone [m³]

ℓ : the distance travelled by the cone [m]

Substituting for 'd' from Eq.5-2 into Eq.5-3 results in an expression for the worn volume of material in terms of load on the grit, the shape of the grit and the sliding distance, and the next Eq.5-4 is obtained.

$$V_g = \frac{2\ell\tan\alpha}{\pi H} \times W_g \qquad \text{(Eq.5-4)}$$

The total wear is the sum of the individual grit worn volumes of the material:

$$V_{tot} = \frac{2\ell\tan\alpha}{\pi H} \times W_{tot} \qquad \text{(Eq.5-5)}$$

where:

V_{tot} : volume of wear loss [m³]

W_{tot} : total load [N]

From this equation, we can understand that the wear loss is closely related to the load and then the hardness is a very important factor to determine the wear resistance.

5.1.2 Comparison of abrasion wear tests

In this research, the relationship between the wear loss and wear distance was investigated in each specimen using Suga abrasion wear tester and Rubber wheel abrasion wear tester. The comparison between Suga and Rubber wheel abrasion wear tests is discussed using the test results of 1% Mo specimen (No.2).

In Suga abrasion wear test, it was found from Fig.4-6 that the wear loss increases proportionally with an increase in wear distance regardless of heat treatment condition. The R_w values, which are expressed by a slope of each straight line, are summarized in Table 4-3. It is found that the R_w value is smallest (0.454mg/m) in the specimen with H_{Tmax}, that is, the specimen has the largest wear resistance, and followed by the as-hardened specimen (As-H:0.481mg/m) with greatest V_γ. The largest R_w or lowest wear resistance was obtained in the specimen tempered at over H_{Tmax} (O-H_{Tmax}:0.510mg/m) which the V_γ was almost nil and the coarsening of secondary carbides occurred.

As for Rubber wheel abrasion wear test, it was found from Fig. 4-7 that the relationship between wear loss and wear distance was similar to that in Suga abrasion wear test and from Table 4-4 that the R_w range from 0.050mg/m to 0.076mg/m. The smallest R_w or largest wear resistance was obtained in As-H specimen and followed by H_{Tmax} specimen. The largest R_w was obtained in O-H_{Tmax} specimen.

When compared with Suga abrasion wear test using specimen with the same heat treatment condition, the R_w value in the Rubber wheel abrasion wear test is much smaller than that of Suga abrasion wear test.

As described in the test wear results, there are a great difference in the wear rate between Suga and Rubber wheel wear tests. It should be understood that this difference causes according to the differences in mechanics of tester, kind and amount of abrasives, applying load and etc., even if an exactly same specimen is used. Therefore, the comparison between two kinds of abrasion tests is discussed under the experimental conditions of this research.

In order to compare the wear rate, the wear loss per unit area (mg/m^2) was calculated for the two types of wear tests using specimen No.2 with heat treatment condition. The calculation method is as follows.

The calculation method of absolute wear loss per unit for Suga abrasion wear test.

In Suga abrasion wear test, the test piece was worn by SiC abrasive paper fixed to aluminum wheel with 12 mm in thickness, and it moving forth by 30 mm and back by 30 mm (one stroke), as shown in Fig.5-2
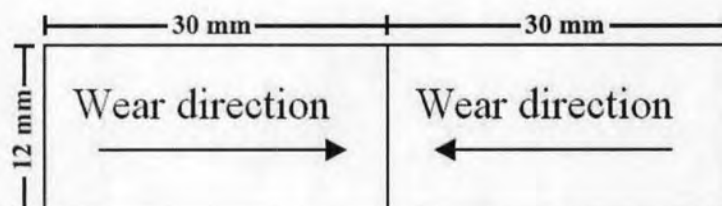

Fig.5-2 Schematic drawing of worn area by 1 stroke, forth and back (Suga abrasion wear test).

Form Fig.5-2, the worn area for 1 stroke is calculated as follows.

The worn area of 1 stroke $=$ 12 x 30 x 2 $=$ 720mm^2

Then, the abrasion wheel is rotated by 0.9 degree to provide the new abrasion surface. After the wheel rotated for 400 times, it completed one revolution or 360 degree. Therefore, the total worn area of one cycle test is obtained as follows.

The worn area of one cycle test $=$ 720 x 400 $=$ 288,000mm^2

After finishing one cycle test, the test piece was cleaned with acetone in an ultrasonic cleaner, dried and measured the weight. Since the test was repeated for eight times in the same test piece, the total worn area is,

The total worn area $=$ 8 x 288,000 $=$ 2,304,000mm^2 $=$ 2.304m^2

Here, the absolute wear loss per unit is obtained by ratio of the total wear loss and the total worn area of eight cycle tests.

The calculation method of absolute wear loss per unit for Rubber wheel abrasion wear test.

In Rubber wheel abrasion wear test, the test piece was worn by silica sands (SiO_2) that are pressed to the surface of test piece by rubber-lined

wheel with 250mm in diameter and 15mm in thickness, as shown in Fig.5-3. The schematic drawing of wheel is shown in Fig.5-4.
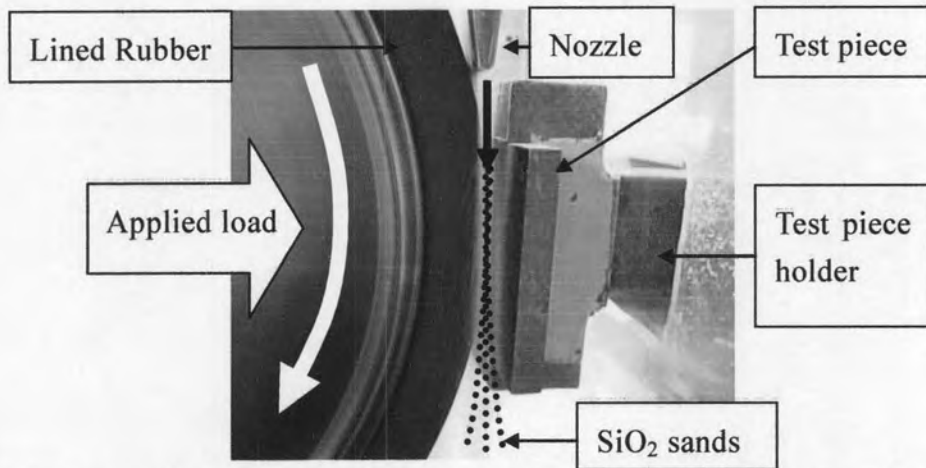

Fig.5-3 Photograph of main portion in wear testing by Rubber wheel abrasion wear tester.
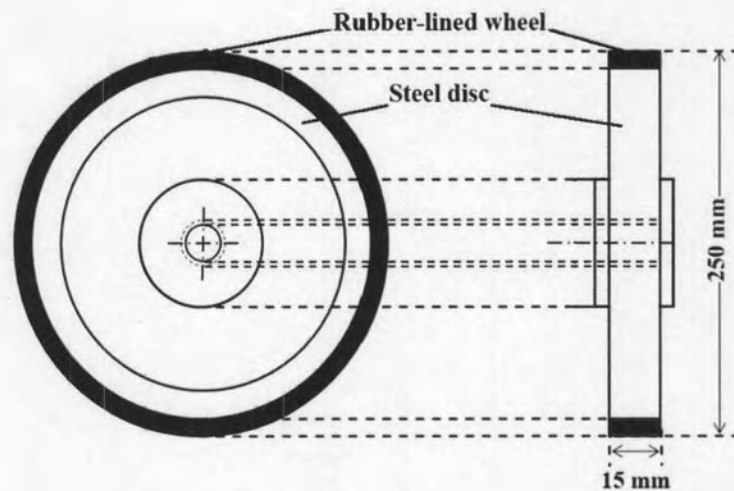

Fig.5-4 Schematic drawing showing Rubber wheel for Rubber wheel abrasion wear test

The test piece was worn by SiO_2 sand being fed in the vacancy between contacting face of test piece and the rubber-lined wheel. The wheel rotates at 120rpm, then the total worn area when the wheel rotates for one revolution is as follows.

The worn area of on revolution $= 2 \times \pi \times \dfrac{250}{2} \times 15 = 11{,}781.0mm^2$

Since the wheel was rotated for 1000 revolutions per one cycle test, the total area of one complete test is as follows.

The total worn area for one complete test = 11,781x1,000 = 11,781,000mm^2

After finishing one cycle test, the test piece was cleaned with acetone in an ultrasonic cleaner, dried and measured the weight. As the test was repeated for four cycles with same specimen, the total worn area was obtained as follows.

The total worn area $= 4 \times 11{,}781{,}000 = 47{,}124{,}000mm^2 = 47.12m^2$

Finally, the absolute wear loss per unit is obtained by ratio of the total wear loss and the total worn area.

The results of calculation for the test pieces heat-treated by different condition are summarized in Table 5-1. In each heat treatment condition, the R_{WT} of Suga abrasion wear test is much greater than that in Rubber wheel abrasion wear test and it is about 10 times. This means that the abrasive wear condition in Suga abrasion wear test is more aggressive than that in Rubber wheel abrasion test. The ratio of R_{WT} is about same in the specimens except for the over-tempered specimen.

Table 5-1 Comparison of absolute wear rate per unit area (R_{WT}) and the ratio of R_{WT} between Suga abrasion wear test and Rubber wheel abrasion wear test. 1% Mo specimen.
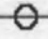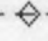
Heat treatment condition	Absolute wear rate per unit area, R_{WT} (mg/m^2) (Total wear loss/Total Worn area)		Ratio (Suga/Rubber)
	Suga	Rubber Wheel	
As-H	40.36	3.29	12.27
B-H$_{Tmax}$	43.19	4.03	10.72
H$_{Tmax}$	38.63	3.95	9.78
O-H$_{Tmax}$	42.75	5.35	7.99
Average			10.19

From above results, it can be said in this experiment that the absolute wear rate per unit area is much larger in Suga abrasion wear test than that in Rubber wheel abrasion wear test. In other word, two-body-type abrasion wear is about 10 times larger than that of three-body-type abrasion wear. It is interesting that in spite of wear test with different test conditions, this result is close to those of research work by M. IÇzciler and H. CËelik [45].

5.1.3 Effect of applied load on wear rate (R_W) in Suga abrasion wear test

It is considered that the R_W related to the condition of wear test, and particularly influenced by the stress or load between the two counterparts. Therefore, the effect of applied load on the wear behavior was investigated using Suga abrasion wear test. The tests were carried out under a load of 0.5, 1 and 3 Kg. The relationship between wear rate (R_W) and applied load is shown in Fig.5-5. The equations of the relationship between R_W and the applied load are shown at the upper part of the figure. Against the applied load or stress, the R_W increases proportionally. This suggests that in the case of Suga abrasion wear test, it is

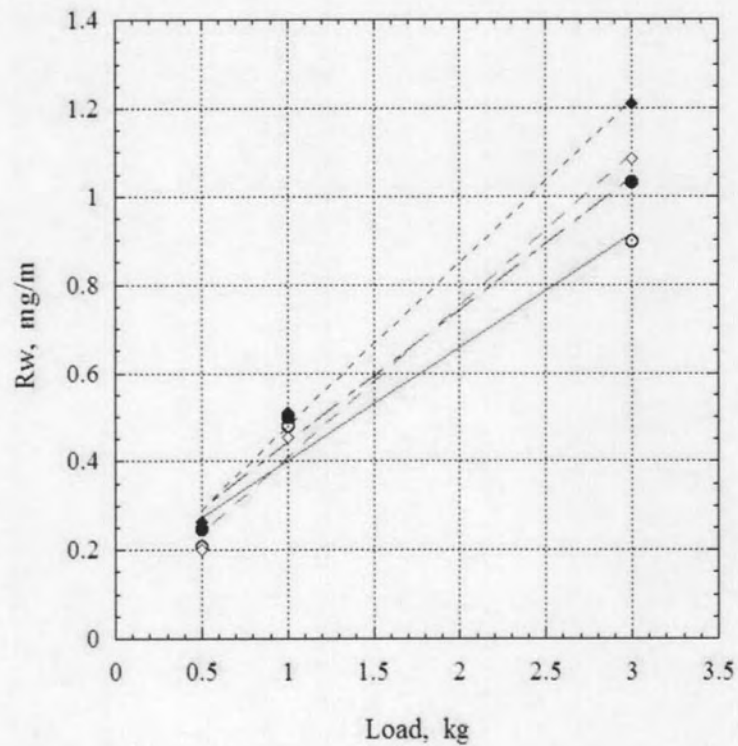| As-H	—⊖—	$W_\ell = 0.257 \times W_d + 0.143$ (R=0.977)
B-H$_{Tmax}$	—●—	$W_\ell = 0.301 \times W_d + 0.141$ (R=0.991)
H$_{Tmax}$	–◇–	$W_\ell = 0.343 \times W_d + 0.065$ (R=0.996)
O-H$_{Tmax}$	--◆--	$W_\ell = 0.371 \times W_d + 0.105$ (R=0.998)

W_ℓ : Wear loss, W_d : Wear distance

Fig.5-5 Relationship between wear rate (R_w) and applied load in 1% Mo specimen by Suga abrasion wear test.

possible for wear resistance of materials to be compared quantitatively by using any applied load. At low applied load, the smallest R_w was obtained in H_{Tmax} specimen followed by the As-H specimen, B-H_{Tmax} specimen and the O-H_{Tmax} specimen and, at higher applied load of 3kg, the smallest R_w was change to As-H specimen followed by the B-H_{Tmax} specimen, H_{Tmax} specimen and the O-H_{Tmax} specimen. The difference in wear rate among the specimen with different heat treatment does not change too much except for that in O-H_{Tmax} specimen which expands a little with an increase in the applied load. The increasing rates of R_w against the applied load are 0.257 in As-H specimen, 0.301 in the B-H_{Tmax} specimen, 0.343 in H_{Tmax} specimen and 0.371 in the O-H_{Tmax} specimen, respectively.

5.2 Correlation between Wear Rate (R_w), Hardness, V_γ and Mo content

5.2.1 Relationship between wear rate (R_w) and hardness

In this study, the effects of macro-hardness on the wear rate (R_w) of Suga and Rubber wheel abrasion wear tests were presented in the Fig.5-6 and 5-7, respectively. From these two diagrams, it is found that the R_w by both of Suga and Rubber wheel abrasion wear tests are within a scattering of 0.1mg/m and 0.03mg/m, respectively and they are roughly proportion to macro-hardness, as the macro-hardness increases. The relation by Suga abrasion wear test is expressed by the next equation,

$$R_w(mg/m) = \{(-6.191 \times 10^{-4}) \times HV\} + 0.9605 \quad (R = 0.7856) \qquad (Eq.5\text{-}6)$$

The same relation of by Rubber wheel abrasion wear test is shown by the following equation,

$$R_w(mg/m) = \{(-2.012 \times 10^{-4}) \times HV\} + 0.2223 \quad (R = 0.7314) \qquad (Eq.5-7)$$

It is clear that the more macro-hardness is, the better wear resistance is obtained. In tempered state, therefore the specimen with H_{Tmax} has the largest wear resistance in both Suga and Rubber wheel abrasion wear tests. To clarify the sensitivity of effect of R_w against an increase in macro-hardness between Suga and Rubber wheel abrasion wear tests, the slope of the trend lines in Fig.5-6 and in Fig.5-7, which are named α_1 and α_2, respectively, are introduced and the ratio of α_1 and α_2 (α_1/α_2) is obtained. The value of α_1/α_2 is 3.08. This means that Suga abrasion wear test has the sensitivity three times as large as that of Rubber wheel abrasion wear test.

Therefore, it is presumed that the macro-hardness, which is taken account of the eutectic carbides, has more effect on Suga abrasion wear test than Rubber wheel abrasion wear test.
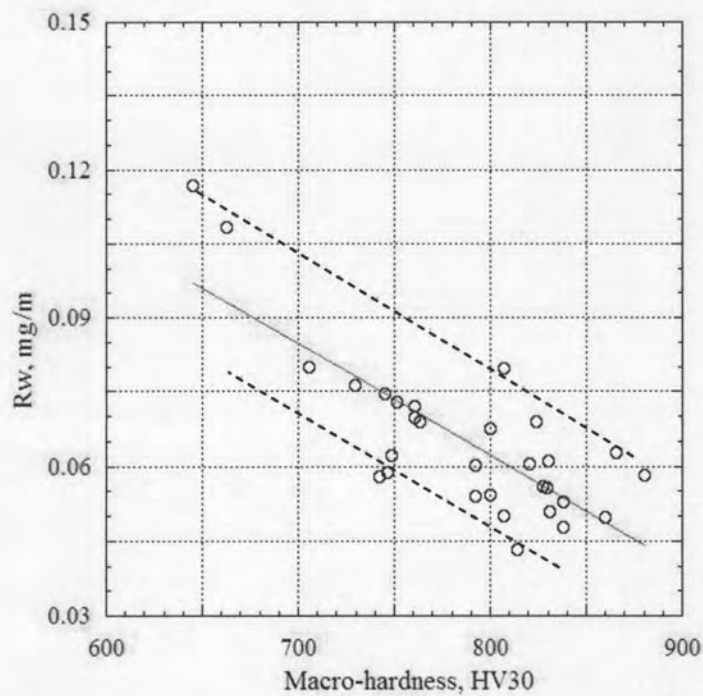
5.2.2 Relationship between wear rate (R_w) and V_γ

The relationship between R_w and V_γ of tested specimens in Suga abrasion wear test and Rubber wheel abrasion wear test are shown in the Fig.5-8 and 5-9. There appears minimum R_w at 15%V_γ for Suga abrasion wear test, and at 10 to 15%V_γ for Rubber wheel abrasion wear test, respectively. This suggests that a certain amount of V_γ could contribute to improve the abrasive wear resistance. These results agree roughly with the experimental results reported by Sare. [7]
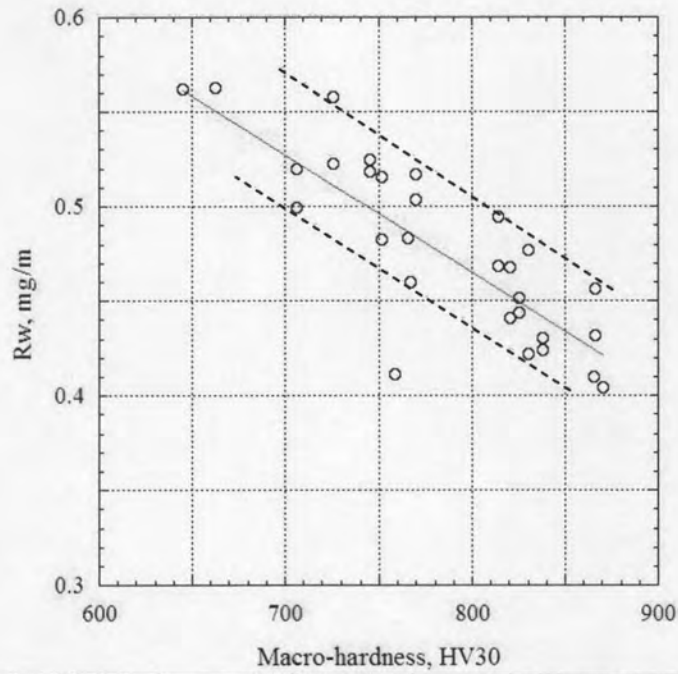
Wear Rate (R_w:mg./m.) = {(-6.191 x 10^{-4}) x HV}+0.9605 (R = 0.7856)---Eq.5-6

Fig.5-6 Relationship between wear rate (R_w) and macro-hardness of specimens without and with Mo, Suga abrasion wear test with a load of 1kg.

Wear Rate (R_w:mg./m.) = {(-2.012 x 10^{-4}) x HV}+0.2223 (R = 0.7314)---Eq.5-7

Fig.5-7 Relationship between wear rate (R_w) and macro-hardness of specimens without and with Mo, Rubber wheel abrasion wear test with a load of 8.7 kg.

In both of Suga and Rubber wheel abrasion wear tests, the R_w decreases remarkably up to 15%V_γ with a decrease in V_γ and over 15%V_γ, it increases gently as the V_γ increases. The decrease in R_w until 15%V_γ is due to an increase of hard martensite and an increase of V_γ to improve the toughness and the precipitation of secondary carbides of M_7C_3 and $M_{23}C_6$ in the matrix.

The reason of gradual increase in R_w when V_γ get over each critical values about 15%V_γ for Suga abrasion wear test and 10-15% V_γ for Rubber wheel abrasion wear test, it is due to that an increase in the V_γ promote the work hardening effect by increased martensite transformation and it contributed the wear resistance. In the area of very low V_γ, the R_w is relatively high in these both two wear tests because matrix is mostly pearlite and coarse secondary carbides.

5.2.3 Relationship between wear rate (R_w) and Mo content

In order to explain the effect of Mo content on the R_w clearly, the relation of R_w and V_γ is are expressed by each specimen and they are shown in Fig.5-10 for Suga abrasion wear test and Fig.5-11 for Rubber wheel abrasion wear test. In Suga wear test, the effect of Mo content on the R_w is clearly shown and it is found that the R_w is decreased or wear resistance is increased with increasing Mo content of specimen and can be said that the V_γ at the minimum R_w shifts to high V_γ side.

However, the R_w in Rubber wheel abrasion wear test does not show clear behavior as that in Suga wear test. In Rubber wheel abrasion wear test, however, it may be certain that the V_γ at the minimum R_w shifts to high V_γ side with an increase in Mo content.
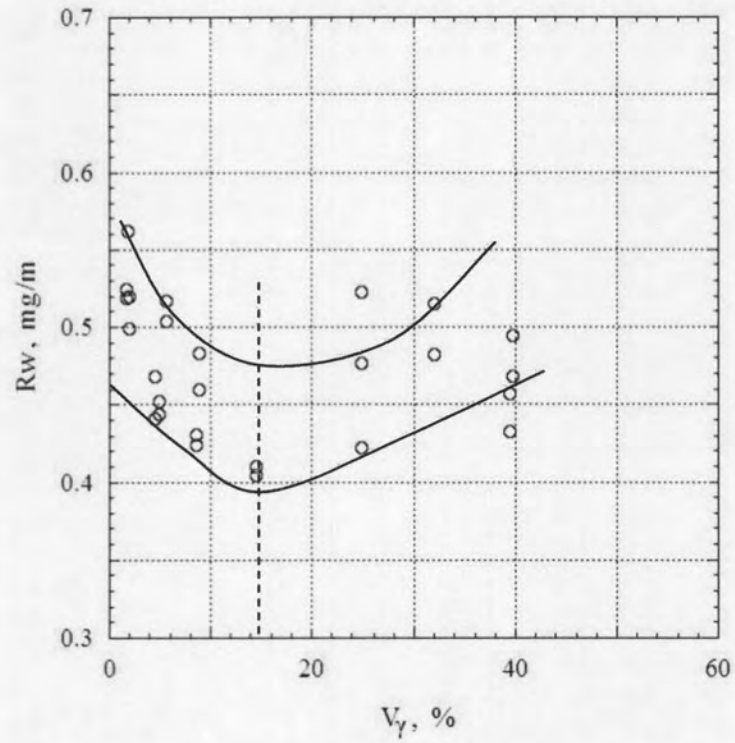
Fig.5-8 Relationship between wear rate (R_w) and V_γ of specimens without and with Mo. Suga wear test with a load of 1kg.
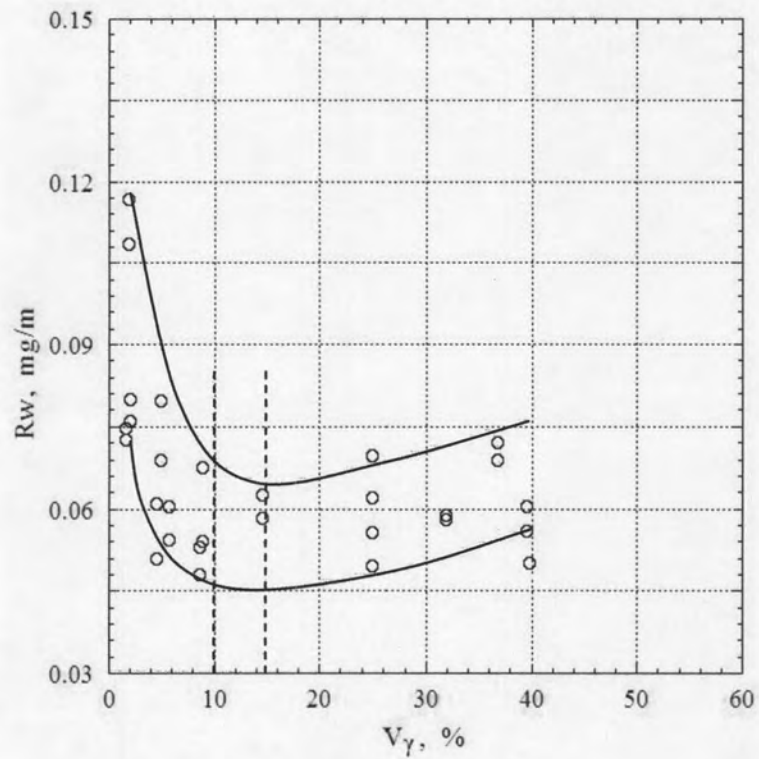

Fig.5-9 Relationship between wear rate (R_w) and V_γ of specimens without and with Mo. Rubber wheel wear test with a load of 8.7 kg.
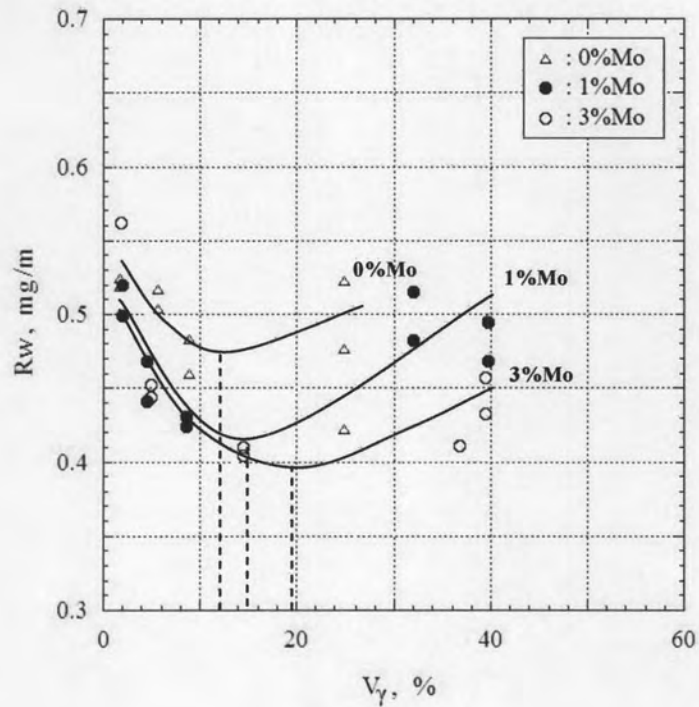
Fig. 5-10 Relationship between wear rate (R_w) and V_γ of specimens No.1, No.2 and No.3. Suga wear test with a load of 1 kg.
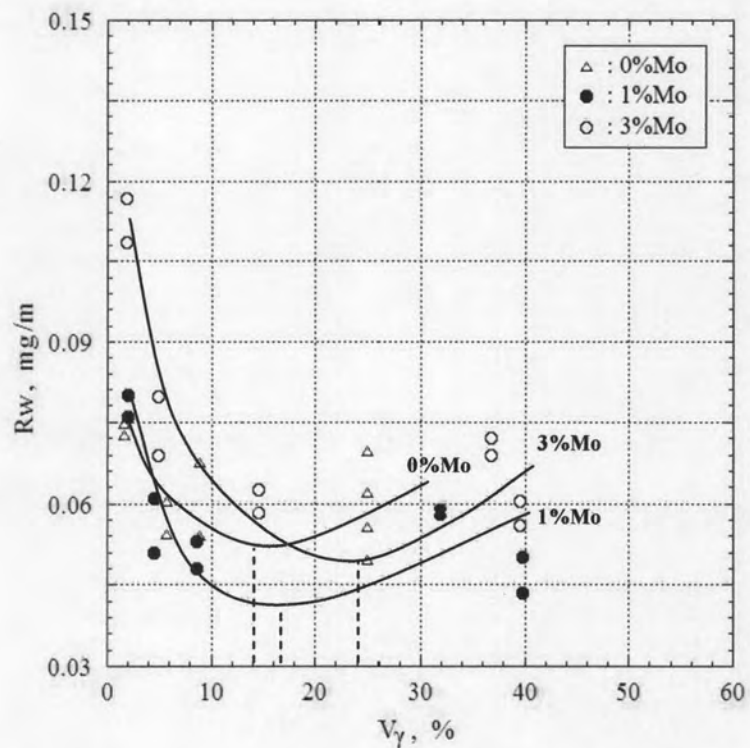

Fig. 5-11 Relationship between wear rate (R_w) and V_γ of specimens No.1, No.2 and No.3. Rubber wheel wear test with a load of 8.7 kg.

5.3 Effect of Oil-quenching on Macro-hardness, Micro-hardness, V_γ and Wear Rate (R_w) of Specimens with H_{Tmax}

Since the final properties of test specimens such as hardness, V_γ and R_w are greatly influenced by the V_γ in the as-hardened state, it is important that the test specimens are hardened enough to transform into martensite or reach the martensite transformation without touching other transformations like the transformations of troostite (fine pearlite) and bainite. To prevent from such imperfect hardening, the specimens hardened by oil quenching were prepared. After hardening the specimens by oil quenching, each specimen was tempered at the temperatures which the H_{Tmax} was obtained in the previous investigation. The heat treatment conditions of wear test pieces are summarized in Table 5-2.

Table 5-2 Heat treatment conditions of oil-quenched specimens.

Heat treatment process	Annealing	Hardening	Tempering
Temperature(K)	1173	1323	748 (No.1) 798 (No.2) 823 (No.3)
Holding time(ks)	18.0	5.4	7.2
Cooling Condition	Furnace	Oil quenching	Fan air cooling

The effect of cooling rate on the macro-hardness and micro-hardness of oil-quenched specimens is shown in Fig.5-13 in which those obtained from specimens cooled by fan air are shown for comparison. It is clear that the H_{Tmax} values of oil-quenched specimens are more in both macro-hardness

and micro-hardness than those of specimens hardened by fan air cooling. The macro-hardness of the oil-quenched specimens are 785.6HV30, 838.3HV30 and 872.7HV30 for specimens No.1, No.2 and No.3, respectively, whereas those of fan-air-cooled specimens are 786.2HV30, 830.7HV30 and 715.5HV30 for specimens No.1, No.2 and No.3, respectively. For the micro-hardness, it shows similar tendency to that of macro-hardness, however, the micro-hardness is overall lower than the macro-hardness. The micro-hardness of fan-air-cooled specimens is 763.4HV0.1, 779.7HV0.1 and 763.58 HV0.1 for specimens No.1, No.2 and No.3, respectively and the micro-hardness of oil-quenched specimens are 765.9HV30, 781.8HV30 and 798.9HV30 for specimens No.1, No.2 and No.3, respectively.

The effect of cooling rate on the V_γ of specimens with H_{Tmax} is shown in Fig.5-14. The V_γ of the oil-quenched specimens are also overall much higher than those of fan-air-cooled specimens that of oil-quenched specimens. The V_γ values of the oil-quenched specimens are 8.84%, 8.54% and 14.55% and those of fan-air-cooled specimens are 5.69%, 4.50% and 4.92% for the specimens No.1, No.2 and No.3, respectively.

Here, the reasons why the micro-hardness, macro-hardness and V_γ of oil-quenched specimens overall higher than those of fan-air-cooled specimens are described. As for hardening, it is considered that the perfect hardening condition, that is the condition of cooling for the specimen not to pass through the transformation of pearlite and bainite, can be obtained by oil quenching. Here, as CCT diagram of a specimen with similar chemical composition to specimen No.3 is introduced and is shown in Fig.5-12. Though the cooling rate of specimens by

oil quenching and fan air cooling were not measure , it can be estimated from the data such as hardness, V_γ and etc. that the cooling rate of oil quenching could be faster than Ⓐ in Fig.5-12 and that of fan air cooling is Ⓑ.
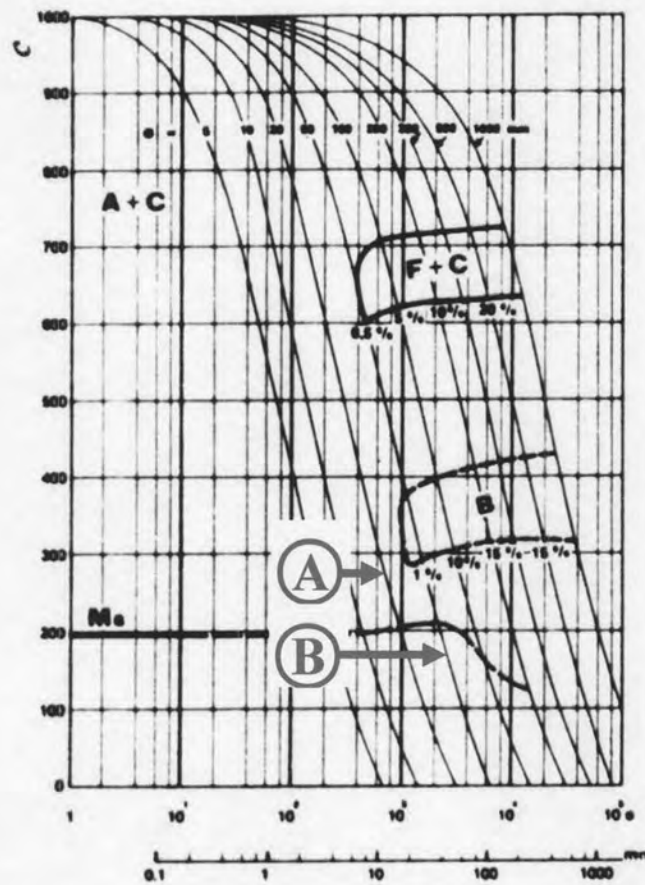

Fig.5-12 CCT diagram for 3.81%C -14.75%Cr – 2.5%Mo.

Fig.5-15 shows the effect of oil quenching for hardening on the R_w by Suga and Rubber wheel abrasion wear tests. The R_w values of the oil-quenched specimens are smaller than those of fan-air-cooled specimens in these two tests. It suggests that the better hardening, or hardening by oil-quenching improves the wear resistance. When the effect of Mo in the specimen is considered, an increase of Mo content also improves the wear
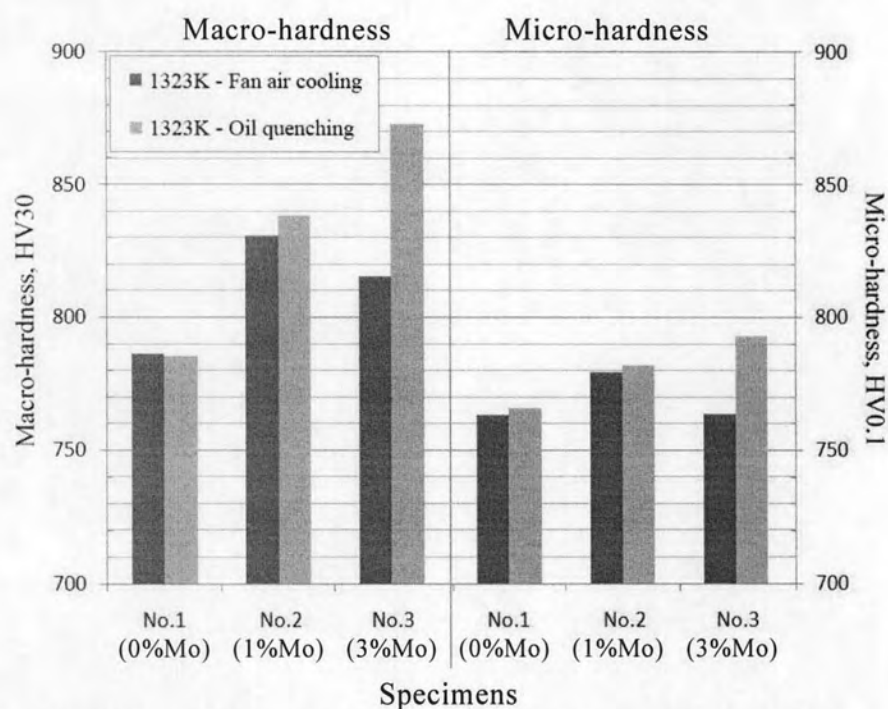
Fig.5-13 Effect of oil quenching on macro-hardness and micro-hardness of specimens tempered at temperatures which give H_{Tmax}.
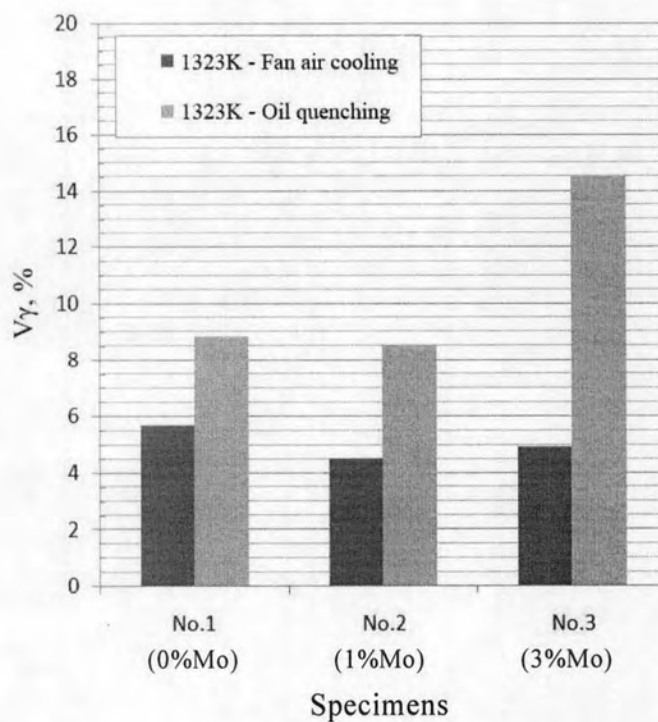
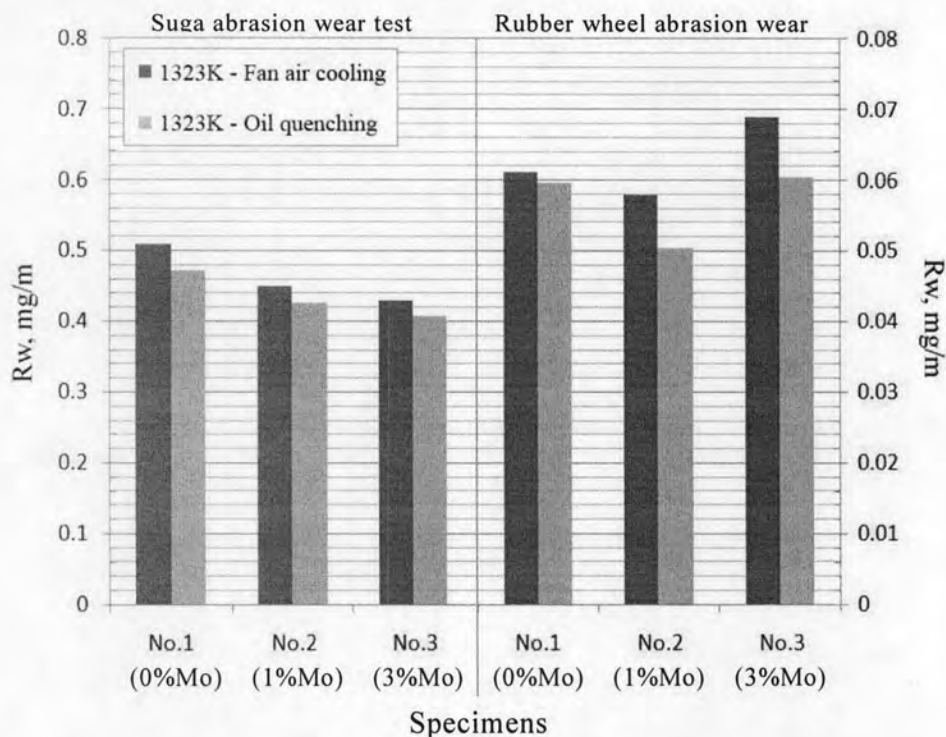Fig.5-14 Effect of oil-quenching on $V\gamma$ of specimens tempered at temperatures which give H_{Tmax}.

Fig.5-15 Effect of oil-quenching on R_W by Suga and Rubber wheel abrasion wear tests of specimens tempered at temperatures which give H_{Tmax}.

resistance in Suga abrasion wear test, however, in Rubber wheel abrasion wear test, the wear resistance of 3%Mo specimen is lower than that of 1%Mo specimen. The reason may be due to the presence of M_2C carbides in 3%Mo that was mentioned earlier in the topic of the effect of wear rate on Mo content.

5.4 Mechanism of Abrasion wear

5.4.1 Suga abrasion wear (Two-body-type abrasion wear)

In the case of Suga abrasion wear test, SiC particles fixed on paper by very strong glue is used. The cross-sectional view is shown in Fig.5-16. The surface of specimen is scratched and cut through by the sharp tips of SiC particles. On all over the surface of specimen, the worn tracks can be clearly seen by SEM
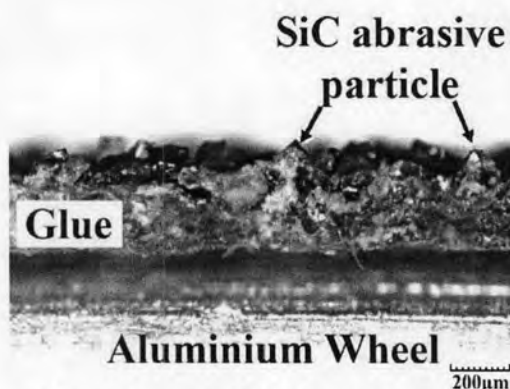
Fig.5-16 Cross-sectional structure of SiC abrasive paper on aluminum wheel for Suga abrasion wear test.

microphotographs.

The cross-sectional microstructures of 1%Mo specimen with H_{Tmax} during wearing are shown in Fig.5-18(a) for the early stage and Fig.5-18(b) for the final stage. It is found that the primary surface is ground an abrasive paper with horizontal movement. The wear progresses on the surface of specimen with flat level by the same abrasives and the same load for each stroke. At the early stage shown in Fig.5-18(a), the matrix is preferably cut off or worn and removed more than the eutectic carbides. Once this phenomenon continues as shown in Fig.5-18(b), cracks possibly occur in the eutectic carbides because the load concentrates on the carbides. Resultantly, spalling of carbides could take place.

To clarify the process of wear, it is helpful investigate the worn surface by comparing it to the cross-sectional microstructure perpendicular to the wear direction. The comparison of both photographs is shown in Fig.5-19. It is understood that the abrasive area of fine lines by scratching on the worn surface corresponds to that of matrix in the microstructure. In the matrix areas that are worn consistently show the fine area in the worn surface. It is also found that the
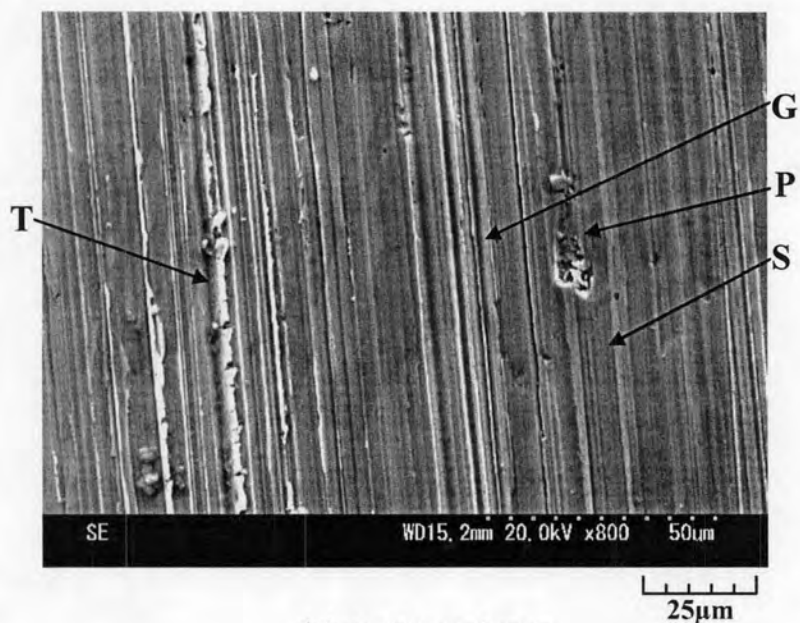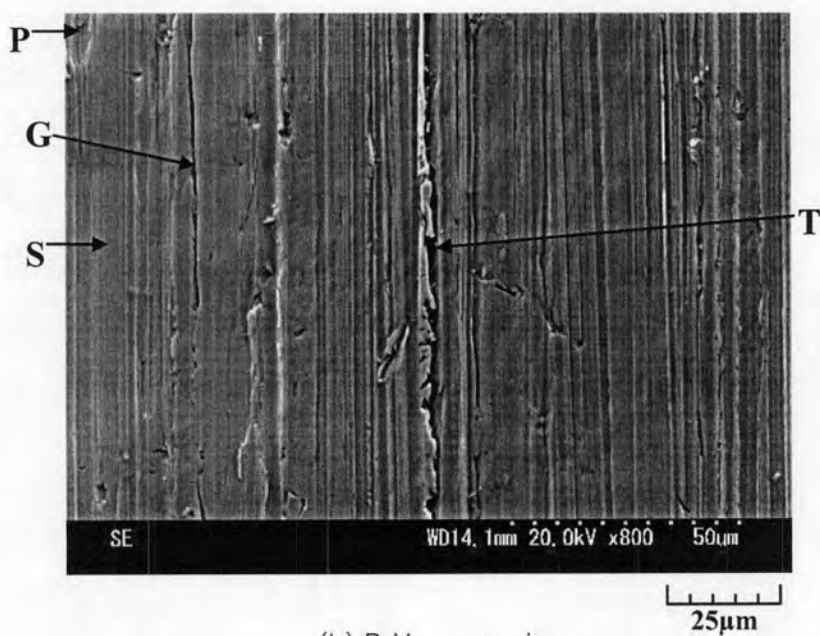
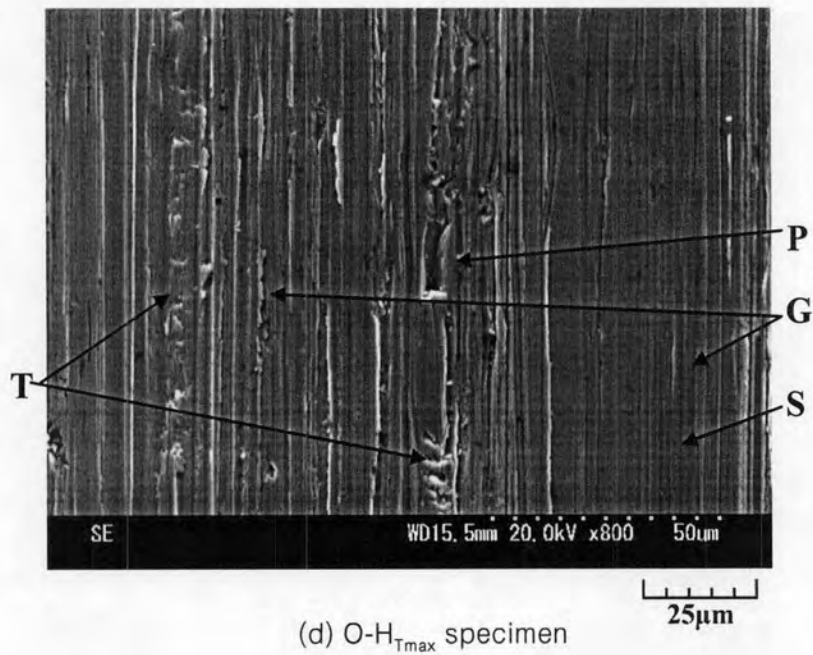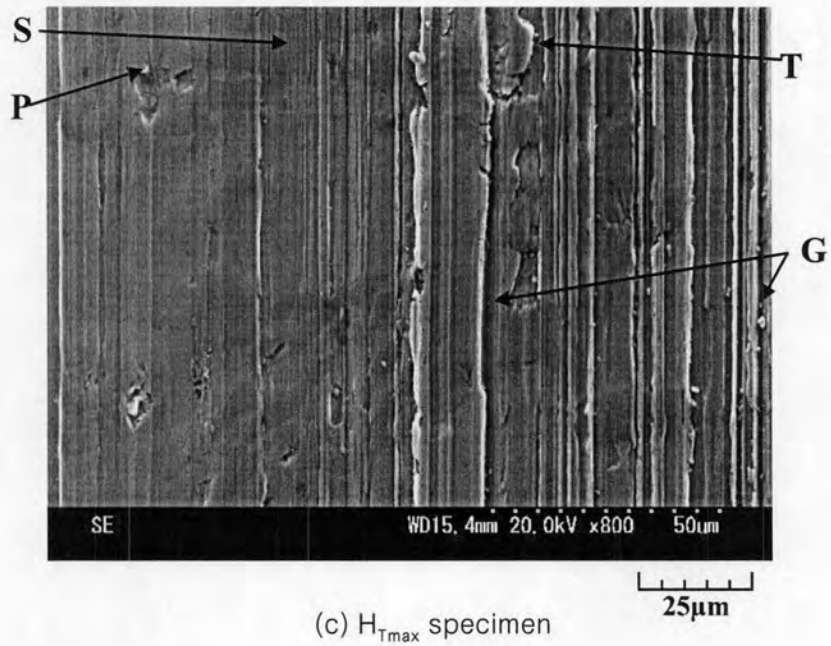(a) As-H specimens

(b) B-H$_{Tmax}$ specimen

Fig. 5-17 SEM microphotographs of worn surfaces of 1%Mo specimens (No.2) with difference heat treatment condition. Suga abrasion wear test with a load of 1kg. (a) As-H specimen and (b) B-H$_{Tmax}$ specimen. S:Scratching, G:Grooving, T:Tearing and P:Pitting.

(c) H_{Tmax} specimen

(d) O-H_{Tmax} specimen

Fig. 5-17 SEM microphotographs of worn surfaces of 1%Mo specimens (No.2) with difference heat treatment condition. Suga abrasion wear test with a load of 1kg. (c) H_{Tmax} specimen and (d) O-H_{Tmax} specimen. S:Scratching, G:Grooving, T:Tearing and P:Pitting.
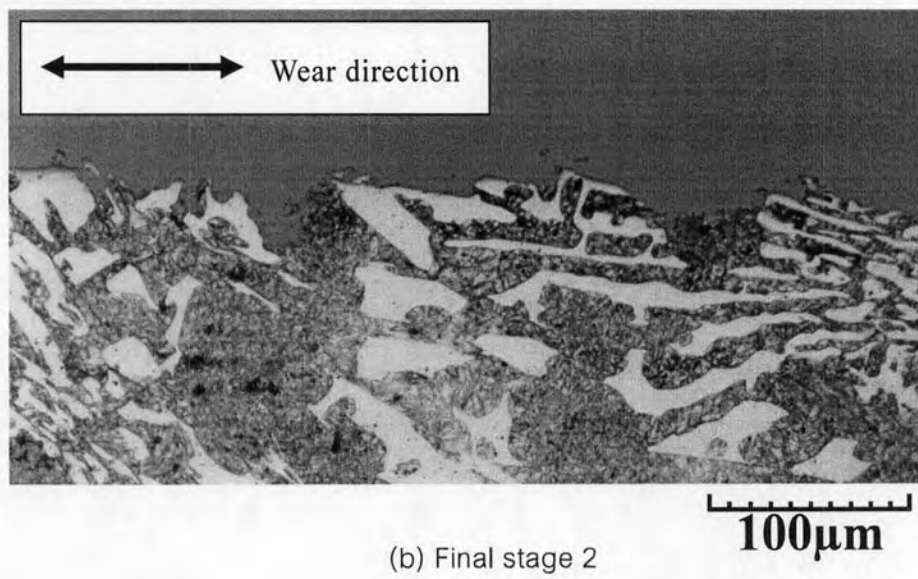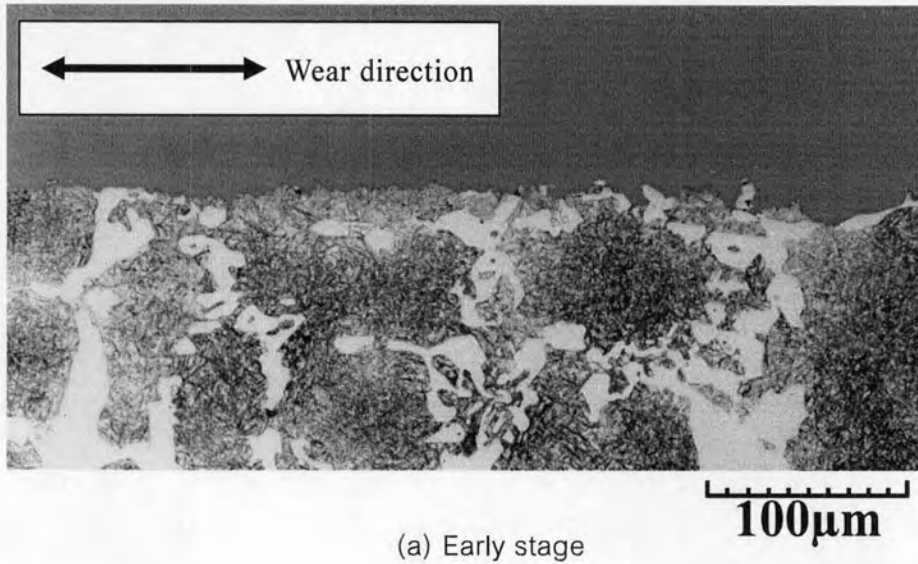
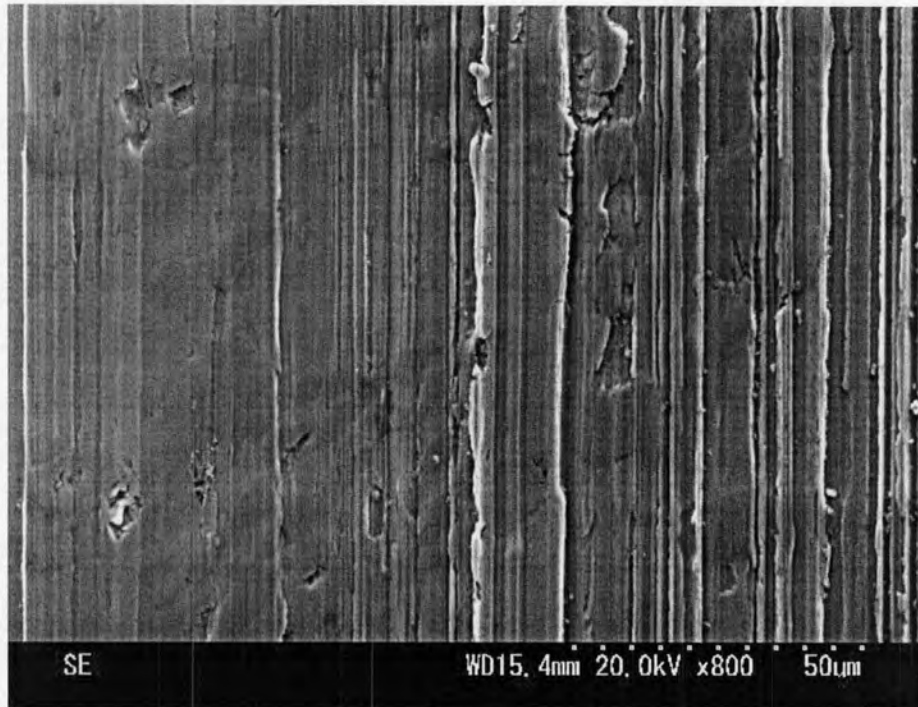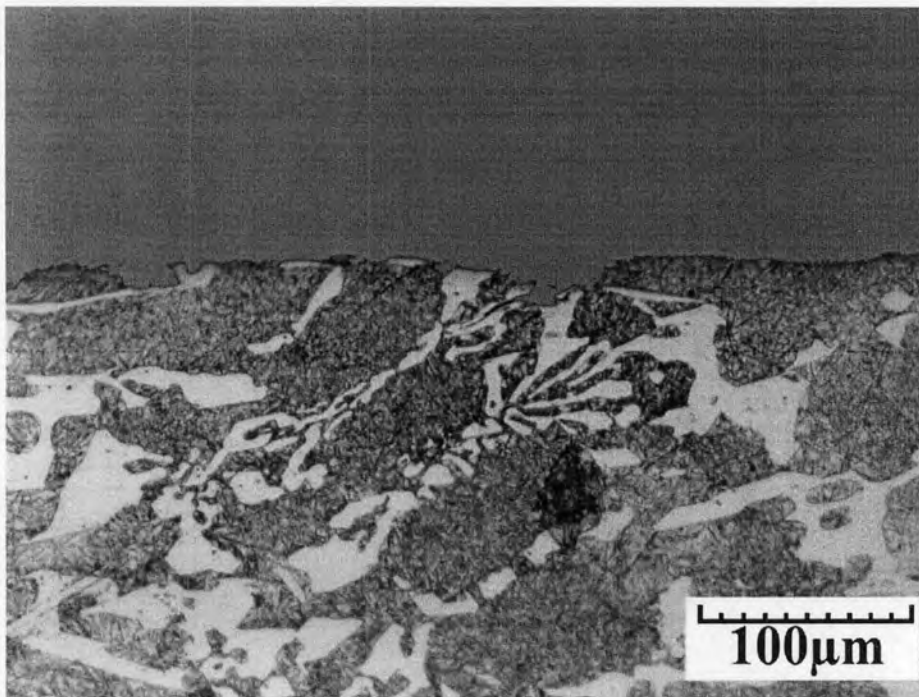(a) Early stage

(b) Final stage 2

Fig. 5-18 Cross-sectional microstructure longitudinal to wear direction to explain the progress of abrasion wear by Suga. (a) Early stage and (b) Final stage.

(a) Worn surface appearance　　25μm

(b) Cross-sectional microstructure near worn surface and perpendicular to wear direction

Fig.5-19 Correspondence and comparison of (a) SEM microphotograph of worn surface and (b) Cross-sectional microstructure by OM perpendicular to wear direction. H_{Tmax} test piece of specimen No.2.

eutectic carbides are worn by scratching and/or spalling in the microphotograph and they correspond to the rougher worn surface by grooving and tearing.
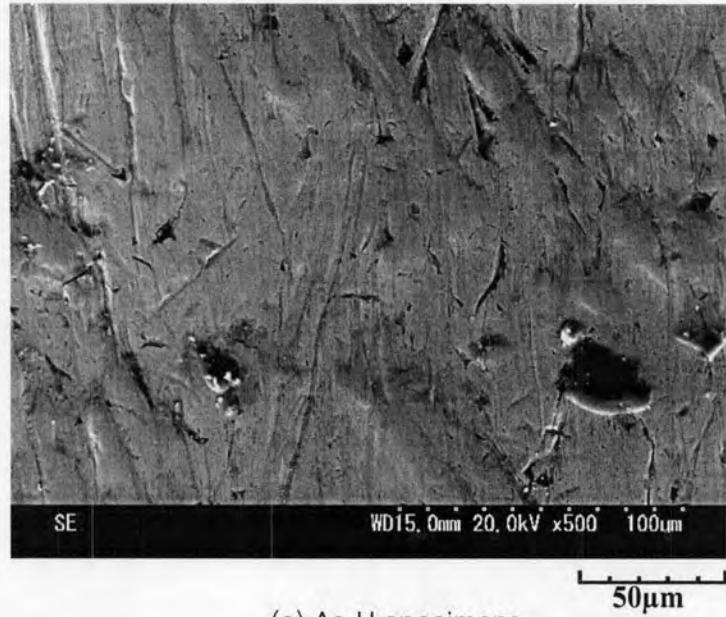
5.4.2 Rubber wheel abrasion wear test (Three-body-type abrasion wear)

From the wear rate (R_w) that was described in Chapter 4, it was found that the best wear resistance was obtained in Ash specimen and the worst wear resistance condition is O-H_{Tmax} specimen. SEM microphotographs of the worn surfaces of 1%Mo specimens with different heat treatment are shown in Fig.5-20(a) to (d). The worn surface of each specimen shows a roundish appearance with tracks in close observation, the matrix is the concave area and the eutectic carbides corresponds to the projection area. This tell that freely rolling SiO_2 sands pass through on the surface of specimen in a high speed by rolling of rubber-lined wheel with pressing a load. Fig.5-22 shows the main portion of wear testing in Rubber wheel abrasion wear tester. , as shown in Fig.5-3. The projection of eutectic carbide area and the crack on the surface can be clearly by SEM microphotographs of the worn surface in Fig.5-20.

Correspondence of the worn surface to the cross-sectional microstructure near the worn surface perpendicular to the wear direction is shown in Fig.5-21. It is clear from the comparison of two photographs that the dendritic matrix areas that were worn selectively are concave and the eutectic carbides that were less worn are projection areas on the worn surface.

Fig.5-22(a) to (c) show the mechanism of progress of wearing by the cross-sectional microstructures. At very early stage of wear the surface is quietly smooth (a). At stage 2 (b), when the test proceed, the surface is worn by SiO_2 sands and the surface has already been indentations In this time, it is clear
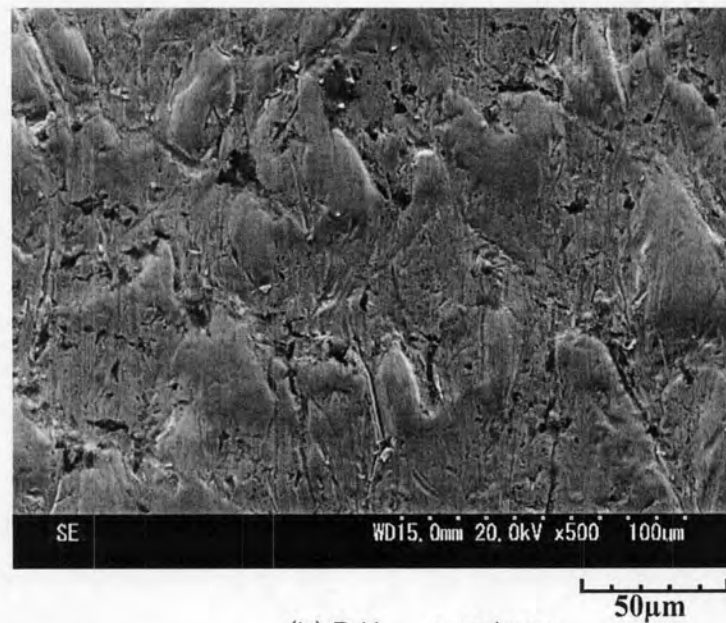
(a) As-H specimens

(b) B-H$_{Tmax}$ specimen

Fig. 5-20. SEM microphotographs of worn surfaces of 1%Mo specimens (No.2) with difference heat treatment condition. Rubber wheel abrasion wear test with a load of 8.7kg. and rolling speed of 120rpm.(a) As-H specimen and (b) B-H$_{Tmax}$ specimen.
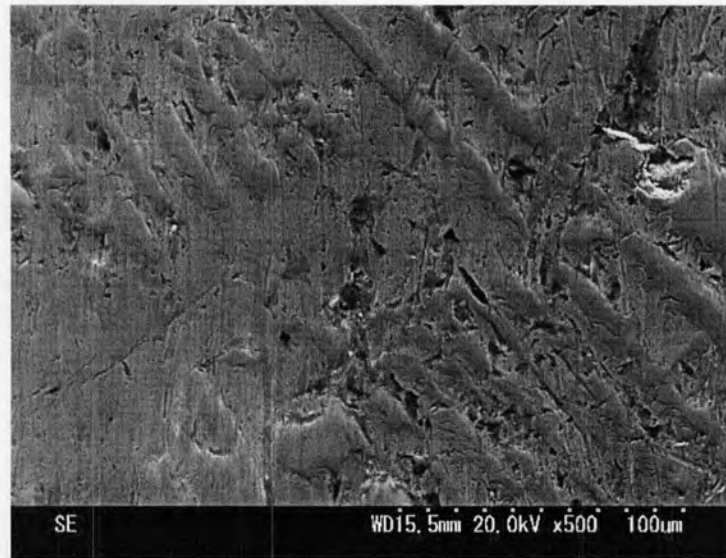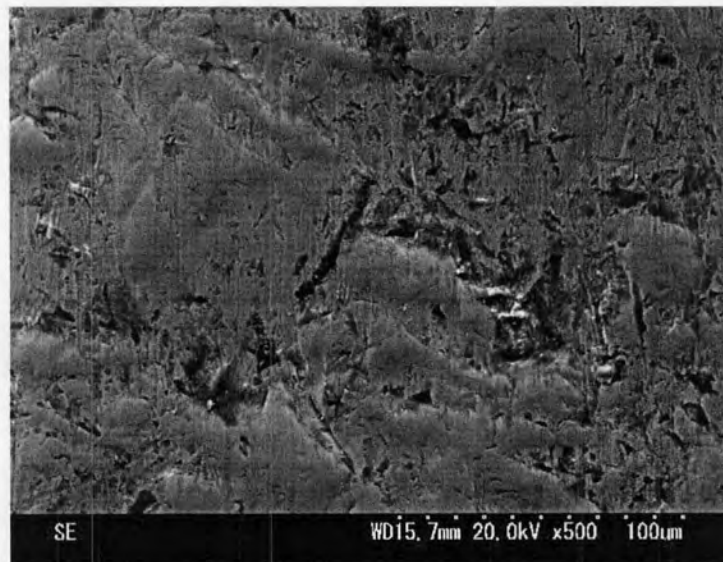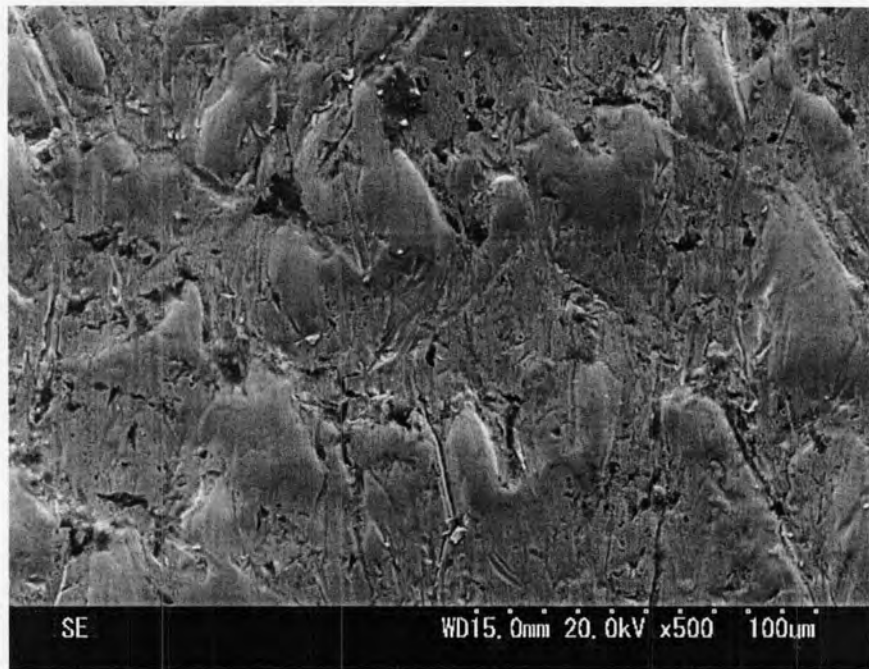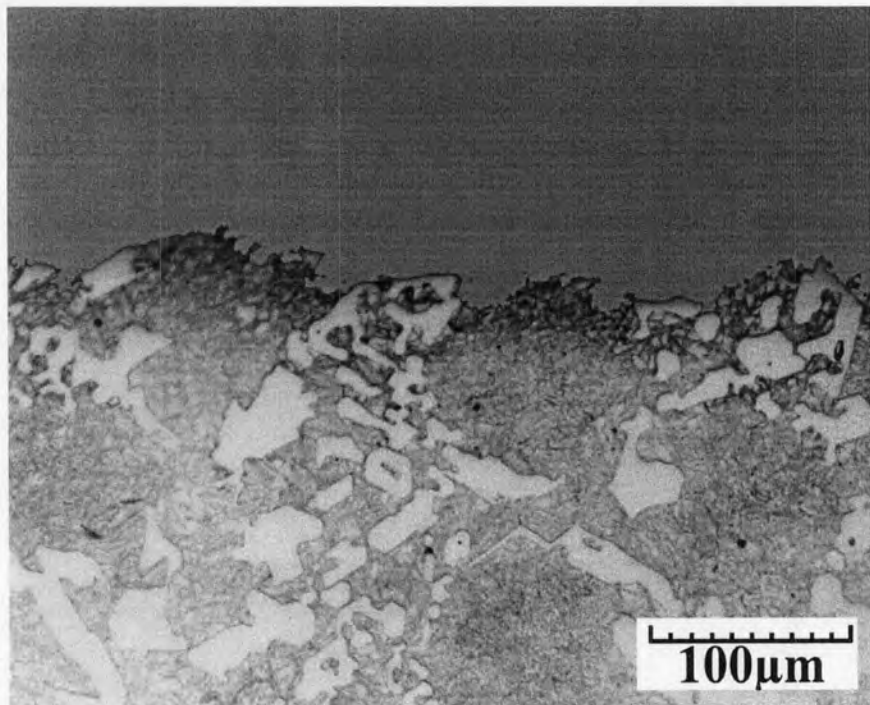
(c) H_{Tmax} specimen

(d) O-H_{Tmax} specimen

Fig. 5-20. SEM microphotographs of worn surfaces of 1%Mo specimens (No.2) with difference heat treatment condition. Rubber wheel abrasion wear test with a load of 8.7kg. and rolling speed of 120rpm.(c) H_{Tmax} specimen and (d) O-H_{Tmax} specimen.

(a) Worn surface appearance

(b) Cross-sectional microstructure near worn surface, perpendicular to the wear direction

Fig.5-21 Correspondence and comparison of (a) SEM structure of worn surface and (b) OM microstructure of cross-sectional near worn surface, perpendicular to the wear direction of H_{Tmax} specimen in Rubber wheel abrasion wear test.

(a) stage 1

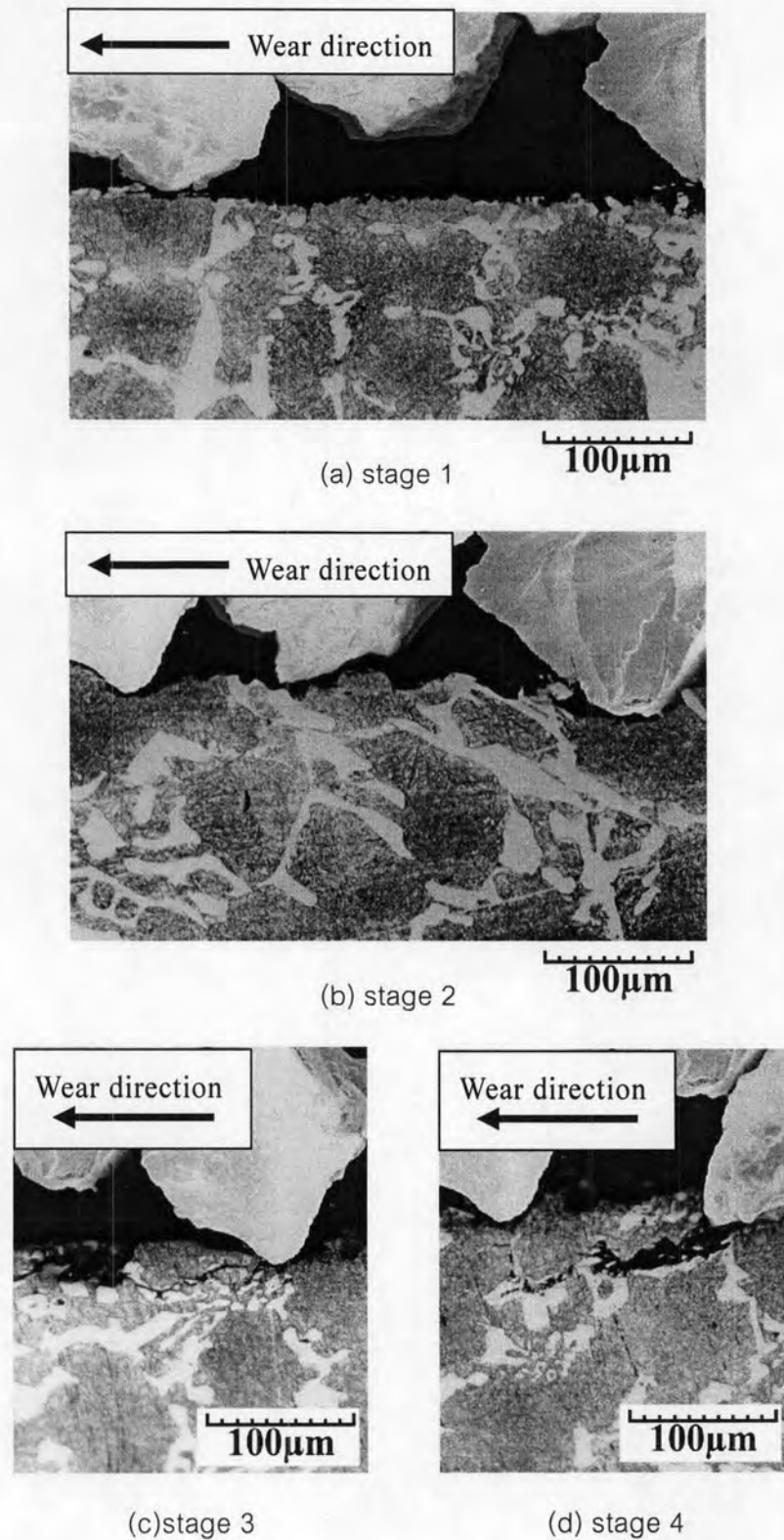(b) stage 2

(c)stage 3   (d) stage 4

Fig. 5-22 Schematic explanation of wear Mechanism by Rubber wheel abrasion wear test using cross-sectional microstructures longitudinal to wear direction. (a) stage 1, (b) stage 2, (c) stage 3 and (d) stage 4.

that the soft matrix is worn more than the hard carbide region, and that the eutectic carbides project from the worn surface, as shown in (b). The microphotograph at stage 3 (c) shows initiation of crack at the portion of the projection with eutectic structure and/or carbide itself. Then, the crack propagation is seen in (d) and later the projection will be worn out or taken away.

From discussion on the progress of abrasion wear by two-body-type abrasion wear (Suga wear test) and in three-body-type abrasion wear (Rubber wheel wear test). It can be clarify that two-body-type abrasion wear by abrasive particles of SiC is much more severe than the three-body-type abrasion wear by those of SiO_2 sands. It is because that, in two-body-type, the abrasive particles are strongly fixed to the ground of the paper and so, so the load or stress is directly applied to the counter surface all over the progressing of test. The similar behavior to this type of wear can be observed in the hot rolling mill rolls and the gears engaged. The abrasives in the former case are scales formed on the surface of hot ingot and those in the latter case are oxides made of gear materials.

To the contrary, the abrasive particles of the three-body-type abrasion wear are not fixed but can roll and move freely. Therefore the stress of wear travels indirectly to the counter surface through abrasive particles and/or from particles to particles to the surface. This behavior of abrasion wear is mainly seen in the pulverizing mills, such as, ball mills for mining and cement industries and vertical mills. In this case, the abrasives are ores and cement clinkers. For the purpose of development of their wear resistance materials, therefore, Rubber wheel abrasion wear test may be more suitable.